Highly Efficient Second-Harmonic Generation in a Double-Layer Thin-Film Lithium Niobate Waveguide

Yuan Li, Lutong Cai* and Lin Zhang*

Key Laboratory of Opto-electronic Information Technology of Ministry of Education and Tianjin Key Laboratory of Integrated Opto-electronics Technologies and Devices, School of Precision Instruments and Opto-electronics Engineering, Tianjin University, Tianjin, 300072, China

**Corresponding author: yuanli_18@tju.edu.cn, lutong_cai@tju.edu.cn, lin_zhang@tju.edu.cn*

Abstract: We demonstrate unprecedentedly efficient second-harmonic generation in a thin-film lithium niobate waveguide, with conversion efficiency as high as 9300% $W^{-1}cm^{-2}$ achieved, which is enabled by greatly enhancing the modal overlap of the higher-order mode in polarization-reversed dual-layer lithium niobate.

1. Introduction

Quadratic nonlinearity ($\chi^{(2)}$) is crucial for many important nonlinear optical processes, including second-harmonic generation (SHG), optical parametric oscillation (OPO), and nonclassical spontaneous parametric down-conversion (SPDC) [1-3]. For high-efficiency $\chi^{(2)}$ nonlinear processes, lithium niobate (LN) is a good candidate due to its high $\chi^{(2)}$ coefficient (d_{33} ~ 25 pm/V) and wide transparent window (0.4–5 μm) [4]. Rapid progresses of wafer-scale thin-film lithium niobate on insulator (LNOI) has been witnessed, because the high refractive-index contrast between the core and cladding leads to tightly confined optical modes and considerably improves the wave-mixing efficiencies in various nonlinear optical processes [5,6]. Quasi-phase matching (QPM) has been successfully implemented in periodically poled LNOI, and a conversion efficiency of up to 4600% $W^{-1}cm^{-2}$ has been reported [7]. An alternative is modal phase matching (MPM), which can avoid technical challenges associated with periodic poling in the QPM scheme [8]. However, the poor modal overlap between modes of different orders in the MPM generally results in low conversion efficiency. Recently, a double-layer LNOI waveguide with a reconfigured $\chi^{(2)}$ profile has been proposed to solve such an issue, but the reported efficiency is still at a comparable level (~5540% $W^{-1}cm^{-2}$) to that of the state-of-the-art QPM LNOI waveguides [9].

Here, we demonstrate that SHG reaches an unprecedented conversion efficiency in a double-layer x-cut LNOI waveguide, which are fabricated with smooth sidewalls, and a record-high normalized conversion efficiency of 9300% $W^{-1}cm^{-2}$ is achieved, associated with an absolute conversion efficiency of 23%. These results hold great potential for developing a variety of important applications, e.g., *f*-2*f* self-referencing for fully integrated self-locked microcombs [10] and high-quality entangled photon generation toward large-scale quantum information processing [11, 12].

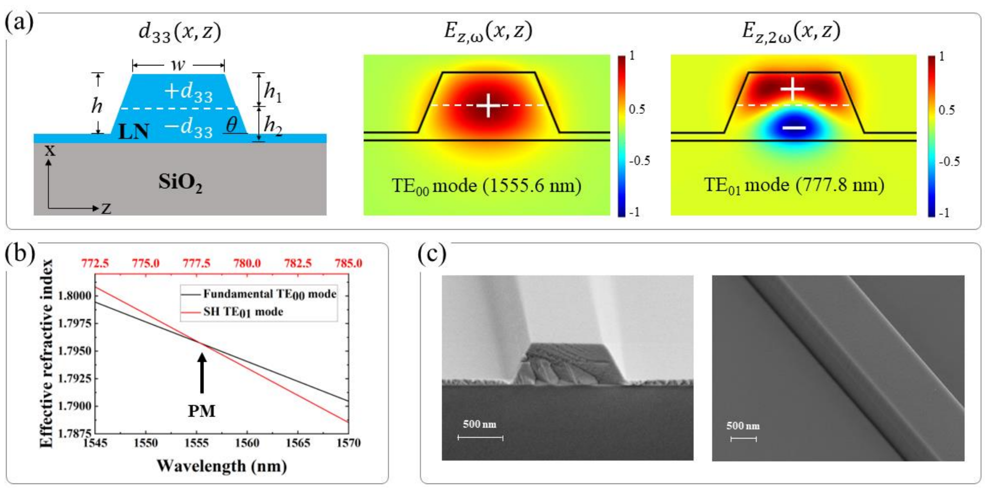

Fig. 1. (a) Schematic of the waveguide cross-section, dominant electric field component (E_z) of the TE_{00} mode at fundamental wavelength and TE_{01} mode at second-harmonic (SH) wavelength. The polarization-reversed double-layer LN with the opposite sign of d_{33} matches the field distribution of the higher-order mode, $E_{2\omega}$. (b) Dependence of the effective refractive indices of the interacting waveguide modes on wavelength. PM occurs at 1555.6 nm. (c) SEM images of the cross-section of the waveguide and waveguide sidewall.

2. Device design and fabrication

To achieve an efficient nonlinear process, the phase matching (PM) condition should be satisfied, which implies:

$$k_{2\omega} = 2k_{\omega} \qquad (1)$$

where k_ω and $k_{2\omega}$ are the wavevectors at fundamental and second-harmonic (SH) frequencies, respectively. Due to the relation of $k = n\omega/c$, Eq. (1) indicates that one needs to find fundamental and SH modes with identical effective refractive indices ($n_\omega = n_{2\omega}$). This can be achieved by selecting the fundamental mode at ω and higher order mode at 2ω.

To utilize the largest component of the second-order nonlinear coefficient ($d_{zzz} = d_{33} = 25$ pm/V), TE_{00} mode at fundamental wavelength and TE_{01} mode at SH wavelength in an x-cut LNOI waveguide are chosen. The cross-section of the double-layer LNOI waveguide is shown in the left panel of Fig. 1(a). The waveguide has a LN film thickness of 500 nm, a top width, w, of 850 nm, an etching depth, h, of 450 nm, and a sidewall angle, θ, of 66.5°. The effective refractive indices of these two modes as a function of wavelength are calculated and shown in Fig. 1(b). The PM condition is achieved at the wavelength of 1555.6 nm. The middle and right panels of Fig. 1(a) show the dominant electric field component (E_z) of the TE_{00} mode at 1555.6 nm and TE_{01} mode at 777.8 nm, respectively. The conversion efficiency of SHG highly depends on the modal overlap integral (Γ):

$$\Gamma = \iint_{LN} d_{33} E_{z,\omega}^2(x,z) E_{z,2\omega}(x,z)\,dxdz \qquad (2)$$

Since the electric field of the higher order mode (i.e., TE_{01} mode in this work) changes its sign across the waveguide core (see TE_{01} mode profile in Fig. 1(a)), the positive and negative contributions to the integral almost cancel out, and the resulting Γ is generally small. However, by introducing a polarization-reversed double-layer structure (see d_{33} distribution in Fig. 1(a)), the nonlinear coefficient d_{33} changes its sign as well across the waveguide, leading to a significant enhancement of Γ and resolving the fundamental issue in the MPM scheme.

The waveguides for SHG are fabricated from an x-cut double-layer LNOI. Each LN layer has a thickness of approximately 250 nm ($h_1 = h_2 = 250$ nm), sitting on 2-μm-thick buried oxide. First, a layer of negative electron-beam resist is spin-coated as the etching mask, and the device patterns are defined by an electron-beam lithography system. Then the patterns are transferred to LN by argon plasma etching in an inductively coupled plasma reactive ion etching (ICP-RIE) tool. The etching depth is measured to be 450 nm. We preserve a 50-nm-thick unetched LN layer to prevent the buried oxide from etching by the hydrofluoric acid in the following cleaning step. The left panel of Fig. 1(c) shows the cross-section of a fabricated waveguide whose geometry is very close to our design. One can see that the two LN layers are tightly bonded together. In particular, as presented in the right panel of Fig. 1(c), the waveguide sidewall is very smooth, implying a low propagation loss. The total length of the waveguide (L) is 2.7 mm.

3. Experimental results

Pump light from a continuous-wave tunable semiconductor laser is coupled into the waveguide using a lensed fiber. We use an in-line fiber polarization controller to ensure TE polarization at the input. When the pump laser is tuned to the PM wavelength, strong SH light can be observed at the waveguide output facet. The SHG signal is collected using an aspheric lens (Numerical Aperture = 0.5) and detected by a photosensor.

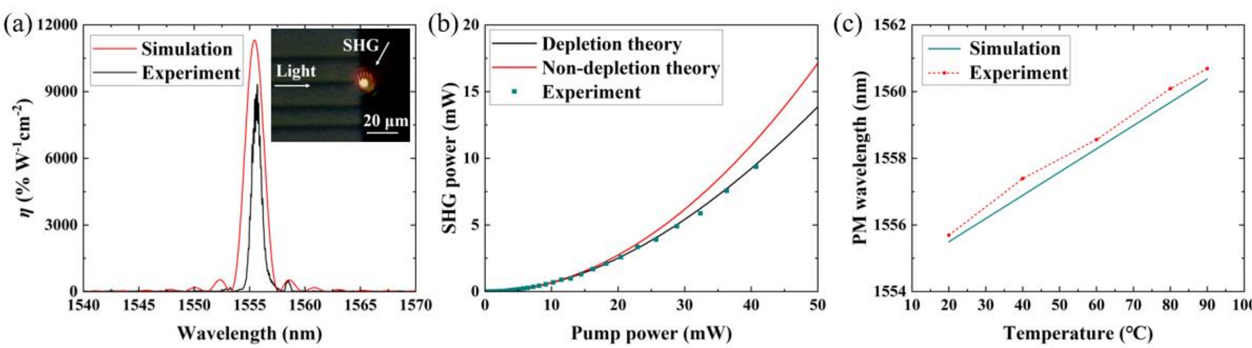

Fig. 2. (a) Experimental (black) and theoretical (red) η as a function of wavelength, Maximum η of 9300% $W^{-1}cm^{-2}$ at 1555.6 nm is observed. (b) Red and black: theoretical dependence of SHG power (at the output facet of the waveguide) on the pump power (at the input facet of the waveguide) under non-depletion and depletion conditions. Green: measured data. (c) Measured and simulated PM wavelengths as a function of temperature, in a good agreement. Also, this exhibits a desirable thermal tunability.

By scanning laser wavelength, we are able to measure the dependence of the SHG signal on wavelength. Taking into account the fiber-to-chip coupling loss (around 9 dB per facet) and assuming that the SHG power generated in the waveguide is completely collected by the lens, the pump power (P_ω) at the input facet and the SHG power ($P_{2\omega}$) at the output facet of the waveguide can be determined. Then, η can be calculated according to the formula: $\eta = P_{2\omega}/(P_\omega L)^2$. We plot η as a function of wavelength in Fig. 2(a). Maximum η of 9300% $W^{-1}cm^{-2}$ at 1555.6 nm is observed, slightly lower than the theoretical value of 11300% $W^{-1}cm^{-2}$. This is associated with an absolute conversion efficiency of 23%. The small discrepancy can be attributed to the uncertainties from the measurement, waveguide propagation losses, and scattering losses arising from the rough waveguide facets (see Fig. 1(c)). The inset is the top-view optical micrograph of the scattered SH signal at the waveguide facet as indicated by the arrow. To the best of our knowledge, this is the highest conversion efficiency reported in LN or LNOI waveguides pumped around the telecommunication band. The main peak of the recorded efficiency spectrum in Fig. 2(a) basically coincides with the theoretical expectation.

By fixing the pump wavelength at 1555.6 nm, where the maximum η locates, the SHG power is recorded as a function of the pump power as shown in Fig. 2(b). As expected, in the low power regime, their relation basically follows a quadratic dependence characteristic of an SHG process. We use an erbium-doped fiber amplifier to further increase the pump power. The discrepancy between the measured SHG power (blue dots) and the theoretical quadratic dependence (red curve) occurs, which is due to the depletion of the pump light when the pump power is high. We modify the model by considering the pump depletion and find that the measured SHG power matches well with the theoretical prediction under pump-depletion condition (black curve).

We leverage the thermo-optic effect in LN to achieve a tunable SHG device. A temperature change would lead to a refractive-index change of LN and thus shift the PM wavelength of the SHG process. Figure 2(c) shows the simulated and measured PM wavelengths as a function of temperature. PM condition moves towards longer wavelengths as the temperature increases. The extracted tunability of the measured result, 0.072 nm K^{-1}, agrees well with simulation, although small discrepancies occur for PM wavelengths at each temperature, which can be attributed to the thermal expansion and pyroelectric effect which are not considered in the simulation model.

4. Conclusion

In conclusion, highly efficient SHG in the double-layer LNOI waveguide is demonstrated. Leveraging the significantly enhanced modal overlap integral in the polarization-reversed LN layers and high-quality nano-fabrication, an on-chip normalized conversion efficiency as high as 9300% $W^{-1}cm^{-2}$ is achieved, associated with an absolute conversion efficiency of 23%, when pumping around 1555.6 nm. Our results lend strong support to the competitiveness of MPM scheme in such a new platform for a variety of nonlinear applications when compared to previously reported methods such as PPLN.

References

[1] R. W. Boyd, A. L. Gaeta, and E. Giese, "Nonlinear Optics," in Springer Handbook of Atomic, Molecular, and Optical Physics, G. W. F. Drake, ed., Springer Handbooks (Springer International Publishing, 2023), pp. 1097–1110.
[2] N. Jornod, M. Jankowski, L. M. Krüger, V. J. Wittwer, N. Modsching, C. Langrock, C. R. Phillips, U. Keller, T. Südmeyer, and M. M. Fejer, "Monolithically integrated femtosecond optical parametric oscillators," Optica 10, 826 (2023).
[3] X. Guo, C. Zou, C. Schuck, H. Jung, R. Cheng, and H. X. Tang, "Parametric down-conversion photon-pair source on a nanophotonic chip," Light Sci Appl 6, e16249–e16249 (2016).
[4] A. Boes, L. Chang, C. Langrock, M. Yu, M. Zhang, Q. Lin, M. Lončar, M. Fejer, J. Bowers, and A. Mitchell, "Lithium niobate photonics: Unlocking the electromagnetic spectrum," Science 379, eabj4396 (2023).
[5] D. Zhu, L. Shao, M. Yu, R. Cheng, B. Desiatov, C. J. Xin, Y. Hu, J. Holzgrafe, S. Ghosh, A. Shams-Ansari, E. Puma, N. Sinclair, C. Reimer, M. Zhang, and M. Lončar, "Integrated photonics on thin-film lithium niobate," Adv. Opt. Photon. 13, 242 (2021).
[6] M. G. Vazimali and S. Fathpour, "Applications of thin-film lithium niobate in nonlinear integrated photonics," Adv. Photon. 4, (2022).
[7] A. Rao, K. Abdelsalam, T. Sjaardema, A. Honardoost, G. F. Camacho-Gonzalez, and S. Fathpour, "Actively-monitored periodic-poling in thin-film lithium niobate photonic waveguides with ultrahigh nonlinear conversion efficiency of 4600 %W^{-1} cm^{-2}," Opt. Express 27, 25920 (2019).
[8] S. Das, B. R. Wenner, J. W. Allen, M. S. Allen, and M. Vasilyev, "Investigation of Hybrid Silicon-Nitride/Polymer Waveguides for Second-Harmonic Generation," IEEE Photonics J. 11, 1–9 (2019).
[9] L. Wang, X. Zhang, and F. Chen, "Efficient Second Harmonic Generation in a Reverse-Polarization Dual-Layer Crystalline Thin-Film Nanophotonic Waveguide," Laser & Photonics Reviews 15, 2100409 (2021).
[10] X. Liu, Z. Gong, A. W. Bruch, J. B. Surya, J. Lu, and H. X. Tang, "Aluminum nitride nanophotonics for beyond-octave soliton microcomb generation and self-referencing," Nat Commun 12, 5428 (2021).
[11] J. Zhao, C. Ma, M. Rüsing, and S. Mookherjea, "High Quality Entangled Photon Pair Generation in Periodically Poled Thin-Film Lithium Niobate Waveguides," Phys. Rev. Lett. 124, 163603 (2020).
[12] L. Cui, H. Feng, X. Zhu, C. Wang, Z. Y. Ou, X. Li, B. E. Little, and S. T. Chu, "Integrated source of telecom-band photon-pairs based on high index silica glass spiral waveguides," in 2023 Optical Fiber Communications Conference and Exhibition (OFC) (IEEE, 2023), pp. 1–3.